ACS Medicinal Chemistry Letters

pubs.acs.org/acsmedchemlett

Letter

Design and Synthesis of Pyrazole-Based Macrocyclic Kinase Inhibitors Targeting BMPR2

Jennifer A. Amrhein, Guiqun Wang, Benedict-Tilman Berger, Lena M. Berger, Amalia D. Kalampaliki, Andreas Krämer, Stefan Knapp,* and Thomas Hanke*

Cite This: *ACS Med. Chem. Lett.* 2023, 14, 833−840

Read Online

ACCESS | Metrics & More | Article Recommendations | Supporting Information

ABSTRACT: Bone morphogenetic protein (BMP) signaling is mediated by transmembrane protein kinases that form hetero-tetramers consisting of type-I and type-II receptors. Upon BMP binding, the constitutively active type-II receptors activate specific type-I receptors by transphosphorylation, resulting in the phosphorylation of SMAD effector proteins. Drug discovery in the receptor tyrosine kinase-like (TKL) family has largely focused on type-I receptors, with few inhibitors that have been published targeting type-II receptors. BMPR2 is involved in several diseases, most notably pulmonary arterial hypertension, but also contributes to Alzheimer's disease and cancer. Here, we report that macrocyclization of the promiscuous inhibitor **1**, based on a 3-amino-1*H*-pyrazole hinge binding moiety, led to a selective and potent BMPR2 inhibitor **8a**.

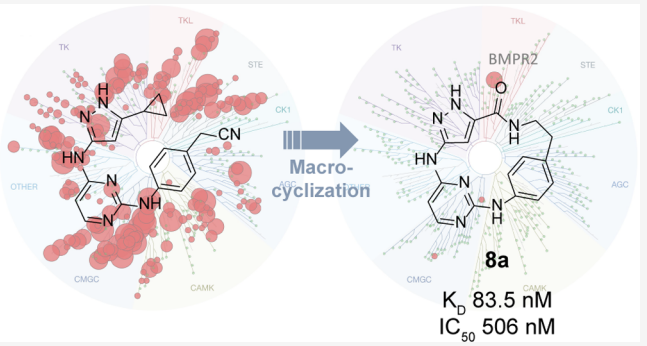

KEYWORDS: *kinase assay, BMPR2, BMP signaling, kinase inhibitor, macrocycle, macrocyclic inhibitor*

The human kinome encodes more than 500 kinases, which have been subdivided into diverse groups and families based on the sequence homology of their kinase domains.[1] Protein kinases catalyze the reversible phosphorylation of specific substrates and are key regulators of cell proliferation, differentiation, metabolism, and apoptosis.[2,3] Dysregulation of these intracellular signaling pathways is responsible for various diseases, in particular cancer.[4] Inhibition of this impaired kinase function by targeting the ATP-binding pocket of the kinase of interest using kinase inhibitors can be used to treat the disease of interest. The major difficulty for conventional type-I and type-II kinase inhibitors is to achieve appropriate selectivity. Macrocyclization of a linear pharmacophore through a linker offers an opportunity to increase the selectivity of the acyclic analogue and provides a relatively new strategy for the development of selective kinase inhibitors.[5] Thus, in recent years, macrocyclization has gained increasing scientific interest in drug discovery and medicinal chemistry. Macrocycles are limited in conformational flexibility, which increases selectivity by providing a locked three-dimensional structure that fits into a kinase of interest and not into other kinase active sites, and this reduces the entropic costs upon binding and provides a higher potency.[6] In addition, biological and physiochemical properties can be tuned by cyclization compared to the acyclic counterpart.[7,8] Furthermore, compared to optimized conventional inhibitors, macrocyclic inhibitors could have lower molecular weight and may have more favorable membrane permeability. Similarly, improved blood−brain permeability was observed for the macrocycle lorlatinib compared with the acyclic analogue crizotinib.[9] The increasing number of drug candidates and the numerous publications in recent years have demonstrated that macrocyclization is an efficient strategy to improve the potency, target selectivity, as well as biochemical properties and offers a great opportunity for the discovery of new drugs.[5,10−12]

The bone morphogenetic protein receptor type-II (BMPR2) is a serine/threonine receptor kinase and belongs to the tyrosine kinase-like (TKL) group. BMPR2, together with diverse type-I receptors, binds bone morphogenetic proteins (BMPs), which are members of the TGF-β superfamily. Binding of these ligands results in the formation of heterotetrameric complexes consisting of two type-I and two type-II receptor homodimers. The type-II dimer activates the type-I complex by phosphorylation at its so-called GS-box.[13] The activated type-I homodimer subsequently phosphorylates R-SMAD proteins (SMADs 1, 5, 8) and activates them, so that

Received: April 11, 2023
Accepted: May 22, 2023
Published: May 30, 2023

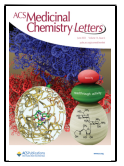

https://doi.org/10.1021/acsmedchemlett.3c00127
ACS Med. Chem. Lett. 2023, 14, 833−840

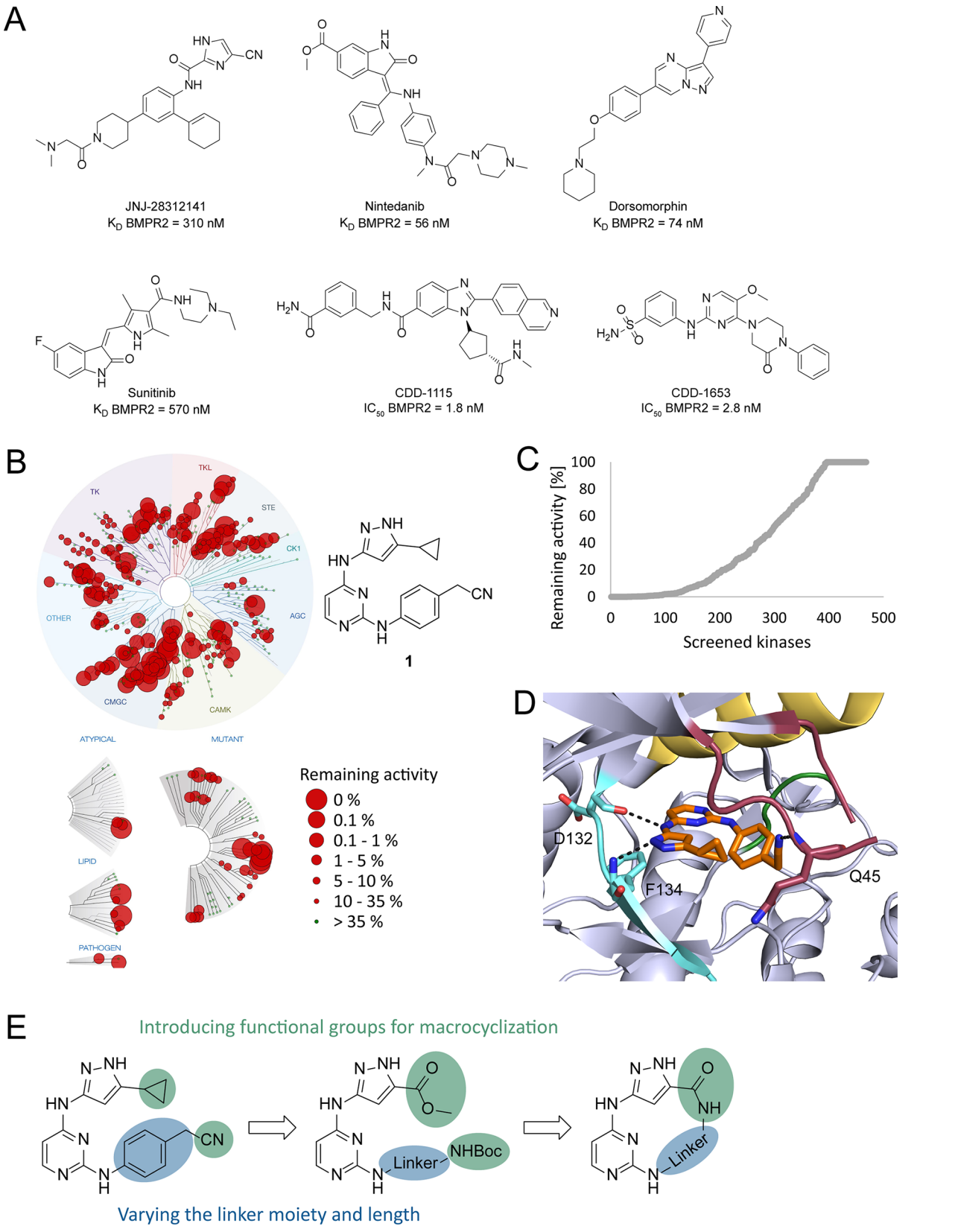

Figure 1. A. Chemical structures of JNJ-28312141, nintedanib, dorsomorphin, sunitinib, CDD-1115, and CDD-1653, with the corresponding K_D and IC_{50} values reported for BMPR2.[23,28,30] B. Selectivity profile of **1** at 1 μM. The chemical structure of **1** is shown beside the dendrogram.[31] C. Waterfall plot of the kinome-wide screening data measured for **1** at 1 μM. D. Compound **1** cocrystallized with VRK1 (PDB: 3OP5).[31,32] The hinge region is colored light blue, the P-loop red, the altered DFG motif green, and the αC-helix yellow, and compound **1** is illustrated in orange. E. Synthetic strategy used for the development of macrocyclic inhibitors based on **1**.

https://doi.org/10.1021/acsmedchemlett.3c00127
ACS Med. Chem. Lett. 2023, 14, 833−840

Scheme 1. Synthesis of the Macrocycles 8a−e[a]

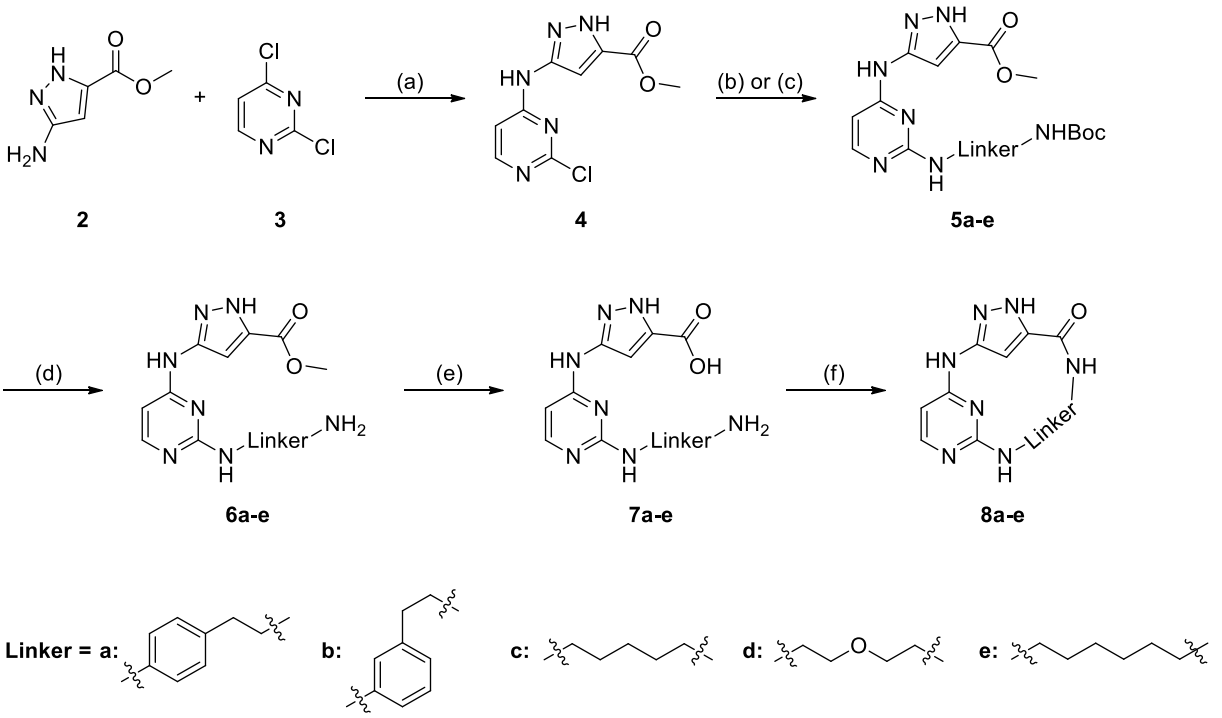

[a]Reagents and conditions: (a) Et_3N, isopropanol, 72 h, 50 °C; (b) Et_3N, ethanol, microwave, 5 h, 120 °C; (c) HCl, ethanol, reflux, 18 h; (d) TFA, DCM, 0 °C to rt, oN; (e) $LiOH{\cdot}H_2O$, THF, H_2O, 18 h, 50 °C; (f) HATU, DIPEA, DMF, 18 h, rt to 70 °C.

they can interact with Co-SMAD (SMAD4). This SMAD heterotrimer complex translocates into the nucleus and regulates the transcription of BMP target genes (Id1−Id4).[14,15] In addition to this canonical signaling pathway, BMPR2 is also involved in noncanonical signaling pathways. For example, BMPR2 is involved in activating the ERK, MAPK, LIMK, NOTCH, and Wnt signaling pathways.[16] BMPR2 expression can be found in many different tissues.[17] It is important for vascular homeostasis, maintenance of pulmonary artery endothelial cell barrier function, and endothelial inflammatory response.[18−20] Impaired BMP signaling has been associated with various diseases such as pulmonary arterial hypertension,[21] vascular pathogenesis,[22] cancer,[23] and Alzheimer's disease.[24,25]

To date, several inhibitors have been described for the type-I receptors, including chemical probes for ALK4/5[26] and ALK1/2.[27] Few inhibitors have been described for the type-II receptor kinases such as BMPR2. Database searches identified only a small number of inhibitors targeting BMPR2 in the nanomolar range. Most of them are promiscuous kinase inhibitors such as JNJ-28312141, sunitinib, and nintedanib, with K_D values of 310, 570, and 56 nM, respectively (Figure 1A).[28] Dorsomorphin, an AMPK inhibitor, also targets BMPR2 with a potent IC_{50} value of 74 nM; however, it also potently affects the type-I receptor kinases ALK2, ALK3, and ALK6 (IC_{50} = 68, 95, and 235 nM, respectively).[23] In 2013, the structure−activity relationship of pyrazolo[1,5-*a*]pyrimidine-based inhibitors derived from the dorsomorphin scaffold was published. These compounds affect BMPR2 in the low nanomolar range, but they also showed potent inhibition of ALK1, ALK2, ALK3, TGFBR2, and VEGFR2.[29] More recently, Modukuri et al. have identified selective benzimidazole-based potent inhibitors (CDD-1115, CDD-1653) of BMPR2 by using a DNA-encoded chemistry technology (Figure 1A).[30]

Compound **1** is a promiscuous kinase inhibitor developed by Statsuk et al. A kinome-wide scan against 468 recombinant human protein kinases emphasized the promiscuous behavior of **1**, which potently inhibits 262 kinases (Figure 1B, C). In this report, type-I and type-II BMP-receptor kinases were potently targeted. Among others, **1** showed strong binding to ALK5 (K_D = 324 nM). The crystal structure in complex with VRK1 revealed an interaction of the 3-aminopyrazole moiety with D132 and F134 of the ATP binding pocket, whereas the pyrimidine faced the hydrophobic pocket (Figure 1D).[31] In this study, we report the development of macrocyclic kinase inhibitors based on the structure of the promiscuous inhibitor **1** to target the understudied type-II receptor kinase BMPR2. To accomplish this, functional groups for the macrocyclization were introduced and different linker moieties were varied (Figure 1E).

The macrocycles **8a−e** were synthesized as shown in Scheme 1. Starting material **2** reacted with 2,4-dichloropyrimidine (**3**) in a nucleophilic substitution to obtain compound **4** with a yield of 16%. Various linkers were attached by a second nucleophilic substitution as previously described.[35] The yields were in a moderate range from 31% to 63%. Cleavage of the Boc-group followed by a saponification with lithium hydroxide led to the precursors **7a−e**. The macrocyclization in the last step was done via an amide coupling, using hexafluorophosphate azabenzotriazole tetramethyl uronium (HATU) to obtain macrocycles **8a−e**.

The synthesized macrocycles were measured in a differential scanning fluorimetry (DSF) assay to investigate their selectivity profile.[33] A positive ΔT_m compared to the ligand-free protein indicates stabilization of the protein by binding of the

https://doi.org/10.1021/acsmedchemlett.3c00127
ACS Med. Chem. Lett. 2023, 14, 833−840

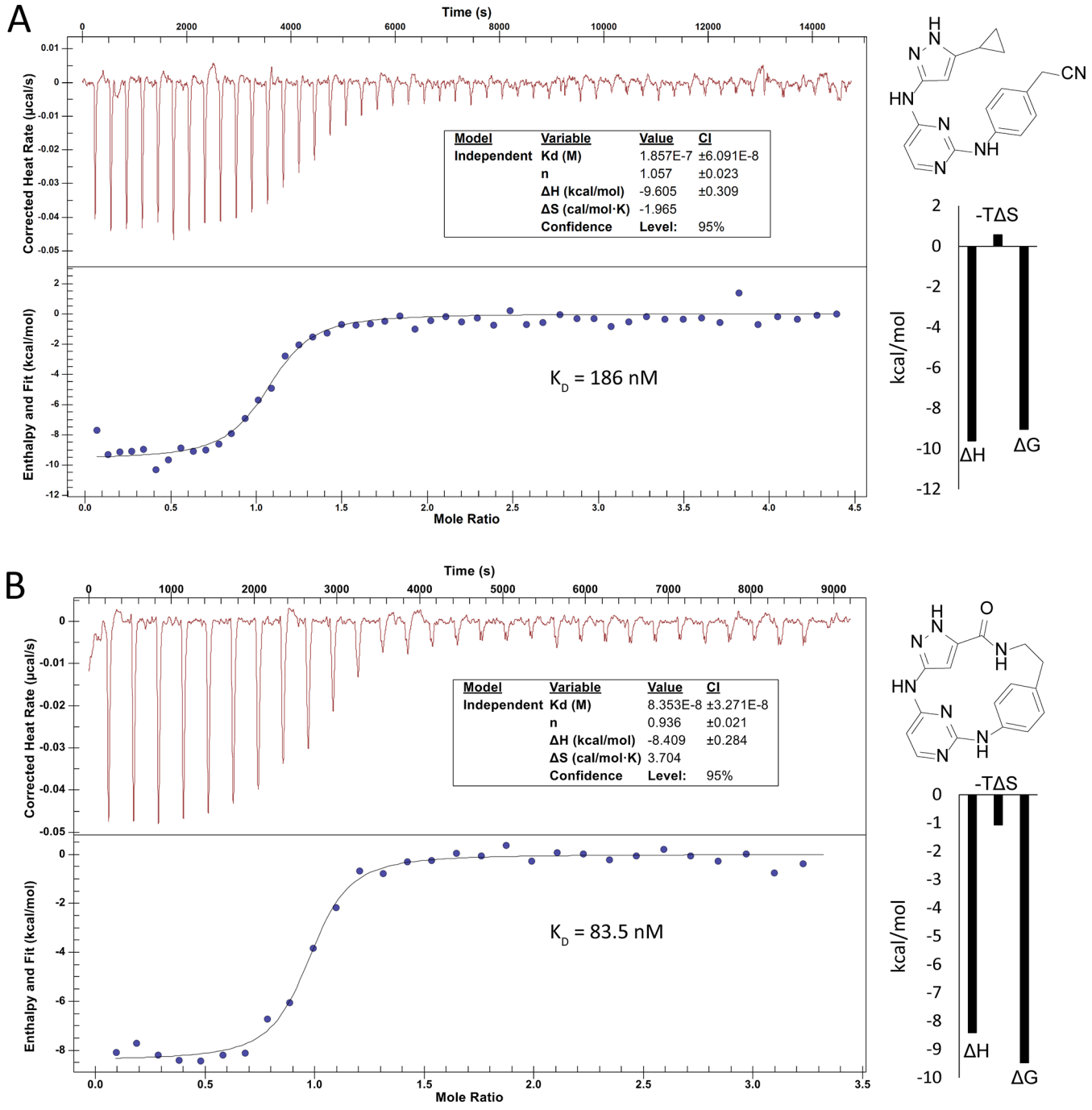

Figure 2. Isothermal titration calorimetry (ITC) data for binding of **1** (panel A) and **8a** (panel B) to the kinase domain of BMPR2 revealed nanomolar binding affinity with K_D values of 186 nM and 83.5 nM, respectively.

compound. For this purpose, an internal panel of 90 kinases was used with staurosporine (**9**) as a positive control. **1** was resynthesized, according to the synthesis published by Statsuk et al.,[31] and its selectivity was assessed using a DSF assay. Macrocycle **8a** showed an interesting profile by binding only three kinases with ΔT_m shifts >5 °C. While its BMP2K binding was negligible compared to that of **9**, GSK3B and BMPR2 were stabilized by **8a** with 8.4 and 5.8 °C, respectively, and were further evaluated. **8b** with an exchanged attachment point on the aromatic linker and **8c** harboring an aliphatic C5 linker appeared to be less selective than compound **8a**, with 17 and 10 stabilized kinases with $\Delta T_m \geq 5$ °C, respectively. Interestingly, even a small change in the linker, from the aliphatic C5 linker in **8c**, replacing a carbon with an oxygen to give compound **8d**, resulted in an inactive compound. By extending the linker by one carbon atom, **8e** regained selectivity compared to **8c**. DSF data revealed stabilization of BMP2K, GSK3B, and STK3 by **8e** with ΔT_m shifts >5 °C, although the ΔT_m shifts were lower compared to those with **9** (Table S1).

Compound **8a** was selected as the most promising candidate for further characterization due to its good stabilization and selectivity, and together with lead structure **1**, the binding affinities were determined by ITC (Figure 2). The ITC data revealed potent binding of compounds **1** and **8a** to BMPR2, with K_D values of 186 nM and 83.5 nM, respectively. However,

https://doi.org/10.1021/acsmedchemlett.3c00127
ACS Med. Chem. Lett. 2023, 14, 833−840

A

Compound	DSF Shift [°C]		ADP Glo™ IC_{50} [nM]	NanoBRET™ IC_{50}		
	BMPR2	GSK3B	BMPR2	GSK3A	GSK3B (intact)	GSK3B (lysed)
1	9.2 ± 0.1	14 ± 0.1	36.2 ± 1.10	4.0 ± 1.0 nM	3.8 ± 0.1 nM	1.2 ± 0.1 nM
8a	5.3 ± 0.1	8.4 ± 0.2	506 ± 70.4	11 ± 2.3 μM	34 ± 1.2 μM	2.3 ± 0.2 μM
8b	5.0 ± 0.1	7.2 ± 0.1	461 ± 17.8	n.d.	n.d.	n.d.
8c	4.6 ± 0.1	4.9 ± 0.4	630 ± 162	> 45 μM	> 45 μM	3.5 ± 1.3 μM

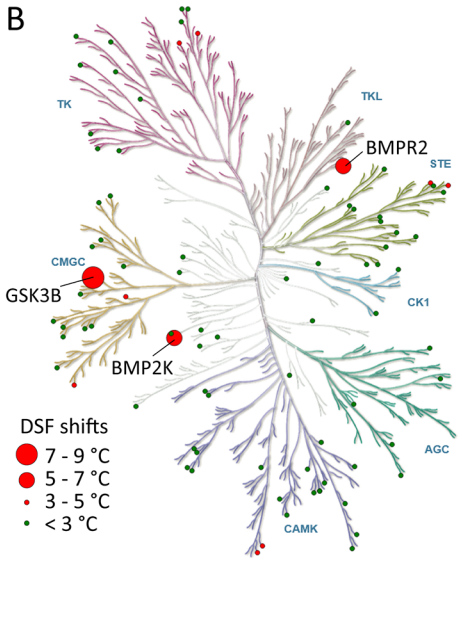

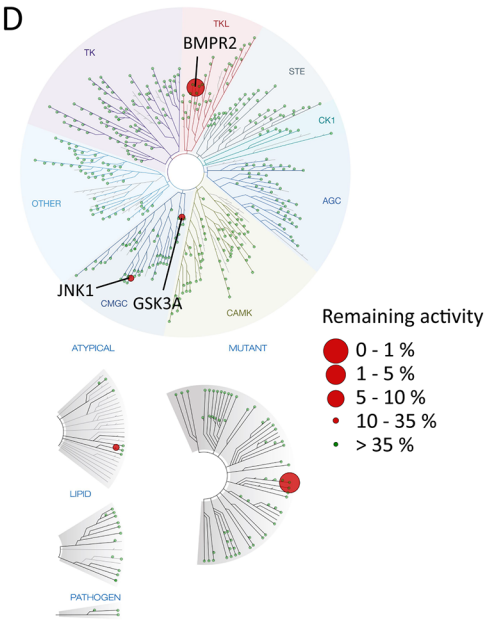

C

Kinase	ΔTm [°C]	% of Reference	K_D Reference [nM]
GSK3B	8.4	71	4.3
BMP2K	5.8	30	1.0
BMPR2	5.3	103*	1500*
FLT1	4.8	36	11
MARK3	4.2	22	0.5
MARK4	3.9	23	0.5
MAPK15	3.8	26	5.5
CDK2	3.8	25	1.3
STK4	3.3	22	1.0
MST3	3.2	44	120
MERTK	3.2	48	6.4

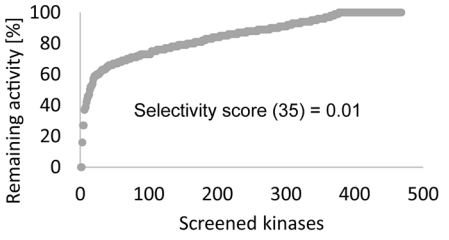

F

Target	Percent of control [%]
FLT3(D835V)	4.5
BMPR2	8.3
GSK3A	16
JNK1	27
RIOK2	27

Figure 3. A. Enzyme kinetic IC_{50} values of **1**, **8a**, **8b**, and **8c** for BMPR2. The values were determined using an ADP-Glo assay. IC_{50} values for GSK3A and GSK3B were determined using NanoBRET. B. Selectivity data of **8a** against an in-house DSF panel of 90 kinases. C. Table summarizing the top hits of the DSF selectivity screen of **8a** as absolute values and with respect to the reference staurosporine. *Lestaurtinib was used as a reference compound. D. Selectivity data of **8a** against a panel of 468 kinases using the KINOMEscan (Eurofins/DiscoverX at 1 μM). E. Waterfall plot illustrating the selectivity of **8a**. F. Top hits of the KINOMEscan of **8a** (for full list see Table S2).

thermodynamic differences between the binding of acyclic lead structure **1** and the macrocycle **8a** could be identified. The binding of **1** was essentially enthalpy-driven (ΔH), balanced by unfavorable binding entropy changes ($T\Delta S$). In contrast, the binding of **8a** was changed by an advantageous entropic contribution ($T\Delta S$) resulting in an overall lower binding constant. The thermodynamic profile suggests that the conformational constraints together with beneficial hydrophobic interactions of the macrocyclic inhibitor resulted in a favorable binding entropy change.

After confirming the binding of macrocycle **8a** to BMPR2 by two orthogonal binding assays, we were more interested in a functional assay, using an ADP-Glo (Promega, Madison, WI, USA) assay to determine the enzymatic inhibition (IC_{50}) values for BMPR2 (Figure 3A). The IC_{50} values of **1**, **8a**, **8b**, and **8c** were in good agreement with the rank order of the measured DSF assay data. Compound **1**, which showed the strongest stabilization in the DSF (9.2 °C), also has the lowest IC_{50} value (36.2 nM) in the ADP-Glo assay. The IC_{50} values for **8a**–**c** ranged from 461 nM to 630 nM (Figure 3A). To determine the potential off-target activity of compounds **1**, **8a**, and **8c**, we screened these compounds in a NanoBRET (Promega, Madison, WI, USA) assay on GSK3A/B (Figure 3A). The promiscuous inhibitor **1** revealed high cellular potency for both off-target kinases, with an IC_{50} value of 4.0 nM. The DSF assay also showed stabilization of GSK3B, with a

https://doi.org/10.1021/acsmedchemlett.3c00127
ACS Med. Chem. Lett. 2023, 14, 833−840

ΔT_m of 8.4 °C for compound **8a**, but this was much less pronounced compared to 14.0 °C for compound **1**. The NanoBRET assay revealed only weak cellular binding for GSK3A/B, with EC_{50} values of 10.9 μM and 33.6 μM. Activity on GSK3B was additionally measured in digitonin-lysed cells to rule out potential cell penetration limitations of the macrocycles. The EC_{50} value on GSK3B in the lysed mode was 2.3 μM for **8a**, while **8c** did not show activity against GSK3A/B, with EC_{50} values >45 μM for both kinases in intact cells. **8c** also showed only weak potency (EC_{50} = 3.5 μM for GSK3B) in the lysed mode (Figure 3A).

After our in-house DSF panel revealed a promising selectivity profile (Figure 3B) and acceptable potency for BMPR2, **8a** was selected for further selectivity profiling, using the ScanMAX KINOMEscan assay platform (Eurofins Scientific) (Figure 3C–E). Gratifyingly, **8a** exhibited exclusive selectivity for BMPR2 in this comprehensive panel, with a selectivity score (S_{35}) of 0.01 (screened at 1 μM). The data confirmed the activity of **8a** at BMPR2, with just a few additional off-targets, e.g., oncogenic FLT mutant, and weak activity for GSK3A, JNK1, as well as RIOK2 (Figure 3C). In addition to the already determined weak activity of macrocycle **8a** on GSK3A/B, we also examined the activity on the two other potential off-targets using the thermal shift assay and NanoBRET assay. Gratifyingly, only a low stabilization of JNK1 and RIOK2 in the thermal shift assay as well as only weak activity in the NanoBRET assay (Table S3) was shown, which confirmed the excellent selectivity profile of **8a**.

To understand the potential binding mode, a docking study was performed with macrocycle **8a** on BMPR2. The docking result revealed an ATP mimetic binding mode of **8a**. The pyrazole moiety formed two hydrogen bonds with the backbone of Y282. A further hydrogen bond was observed between the amine linking the pyrimidine moiety and the aromatic ring with the backbone oxygen of the residue S350. Additional hydrophobic interactions have been noticed with I209, V217, and L340. The choice of the sterically demanding linker in compound **8a** presumably forces the three aromatic ring systems out of planarity, leading to a strong ring strain of the macrocycle and reducing the flexibility to adopt different conformations (Figure 4). Unfortunately, attempts to cocrystallize BMPR2 with **1** or **8a** failed, preventing us from determining experimental structures of **1** and **8a**.

In summary, we have developed a novel series of macrocyclic kinase inhibitors possessing a 3-amino-1*H*-pyrazole scaffold, derived from the highly promiscuous kinase inhibitor **1**. Rigidization using a macrocyclic approach of the 3-amino-1*H*-pyrazole scaffold with different linkers allowed us to strongly manipulate the selectivity profile of the promiscuous kinase inhibitor **1**. With the aromatic linker in compound **8a**, we developed a potent (IC_{50} = 506 nM) and selective BMPR2 inhibitor. Using ITC, we were able to show that the binding was enthalpically and entropically driven, whereas compound **1** exhibited mainly enthalpically driven binding to BMPR2. A docking study supports the result in which an ATP mimetic interaction with the hinge was observed. The docking model suggested that we succeeded in rotating the two heterocycles out of the planarity expected in their open form. This conformation was enforced by a short and rigid linker present in compound **8a**. In this study, we demonstrated that macrocyclization is a powerful tool to enhance the selectivity profile of unselective acyclic compounds. Compound **8a** represents a promising starting point that requires further

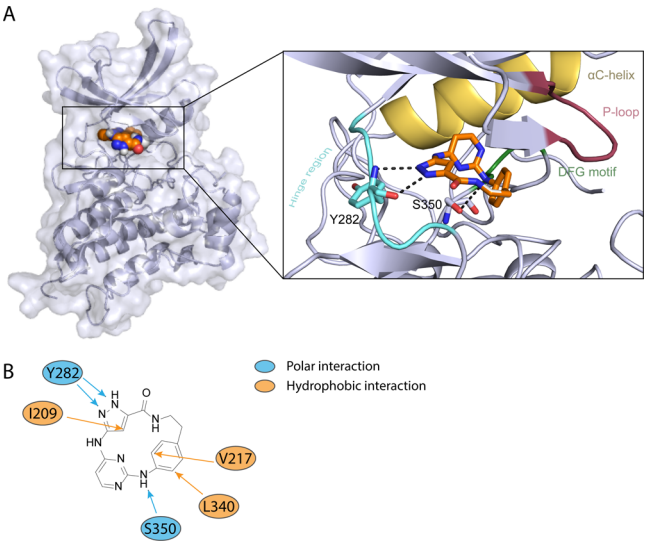

Figure 4. A. Binding mode of **8a** with the kinase domain of BMPR2 determined by *in silico* docking. Macrocycle **8a** was docked into the active conformation of BMPR2 (PDB: 6UNP). Hinge region is highlighted in light blue, P-loop red, DFG motif green, and αC-helix yellow, and the compound **8a** is illustrated in orange. Docking poses were viewed by PyMOL, and protein–ligand interactions were analyzed using the PLIP.[34] B. Interactions between the inhibitor and the amino acid residues of the protein kinase. Blue indicates a polar interaction and orange a hydrophobic interaction between the inhibitor **8a** and BMPR2.

characterization to better assess its potential in the cellular context, as the data so far are all *in vitro* data for BMPR2. The recently published compounds CDD-1115 and CDD-1653 are also very potent and selective *in vitro* compounds; however, there was a large discrepancy between the *in vitro* IC_{50} values and the *in cellulo* activity. Here, macrocycle **8a** represents an additional chemotype that would be worth evaluating in the same context, to see if the discrepancy between the *in vitro* and *in cellulo* data is related to the compounds or is a target-related effect. Nonetheless, at this point we have identified a potent and selective BMPR2 inhibitor that represents an encouraging *in vitro* tool compound.

■ ASSOCIATED CONTENT

Supporting Information

The Supporting Information is available free of charge at https://pubs.acs.org/doi/10.1021/acsmedchemlett.3c00127.

Details of preparation, characterization, and evaluation experiments of compounds **4**–**8** (PDF)

■ AUTHOR INFORMATION

Corresponding Authors

Thomas Hanke − *Institute for Pharmaceutical Chemistry, Johann Wolfgang Goethe-University, D-60438 Frankfurt am Main, Germany; Structure Genomics Consortium, Buchmann Institute for Molecular Life Sciences, Johann Wolfgang Goethe-University, D-60438 Frankfurt am Main, Germany;* orcid.org/0000-0001-7202-9468; Phone: (+49)69 798 29313; Email: hanke@pharmchem.uni-frankfurt.de

Stefan Knapp − *Institute for Pharmaceutical Chemistry, Johann Wolfgang Goethe-University, D-60438 Frankfurt am Main, Germany; Structure Genomics Consortium, Buchmann Institute for Molecular Life Sciences, Johann Wolfgang*

https://doi.org/10.1021/acsmedchemlett.3c00127
ACS Med. Chem. Lett. 2023, 14, 833–840

Goethe-University, D-60438 Frankfurt am Main, Germany; German Cancer Consortium (DKTK), German Cancer Research Center (DKFZ), 69120 Heidelberg, Germany; orcid.org/0000-0001-5995-6494; Phone: (+49)69 798 29871; Email: knapp@pharmchem.uni-frankfurt.de

Authors

Jennifer A. Amrhein − *Institute for Pharmaceutical Chemistry, Johann Wolfgang Goethe-University, D-60438 Frankfurt am Main, Germany; Structure Genomics Consortium, Buchmann Institute for Molecular Life Sciences, Johann Wolfgang Goethe-University, D-60438 Frankfurt am Main, Germany*

Guiqun Wang − *Institute for Pharmaceutical Chemistry, Johann Wolfgang Goethe-University, D-60438 Frankfurt am Main, Germany; Structure Genomics Consortium, Buchmann Institute for Molecular Life Sciences, Johann Wolfgang Goethe-University, D-60438 Frankfurt am Main, Germany; German Cancer Consortium (DKTK), German Cancer Research Center (DKFZ), 69120 Heidelberg, Germany;* orcid.org/0000-0003-2896-3928

Benedict-Tilman Berger − *Institute for Pharmaceutical Chemistry, Johann Wolfgang Goethe-University, D-60438 Frankfurt am Main, Germany; Structure Genomics Consortium, Buchmann Institute for Molecular Life Sciences, Johann Wolfgang Goethe-University, D-60438 Frankfurt am Main, Germany;* orcid.org/0000-0002-3314-2617

Lena M. Berger − *Institute for Pharmaceutical Chemistry, Johann Wolfgang Goethe-University, D-60438 Frankfurt am Main, Germany; Structure Genomics Consortium, Buchmann Institute for Molecular Life Sciences, Johann Wolfgang Goethe-University, D-60438 Frankfurt am Main, Germany;* orcid.org/0000-0002-7835-8067

Amalia D. Kalampaliki − *Department of Pharmacy, Division of Pharmaceutical Chemistry, National and Kapodistrian University of Athens, 15771 Athens, Greece*

Andreas Krämer − *Institute for Pharmaceutical Chemistry, Johann Wolfgang Goethe-University, D-60438 Frankfurt am Main, Germany; Structure Genomics Consortium, Buchmann Institute for Molecular Life Sciences, Johann Wolfgang Goethe-University, D-60438 Frankfurt am Main, Germany; German Cancer Consortium (DKTK), German Cancer Research Center (DKFZ), 69120 Heidelberg, Germany*

Complete contact information is available at: https://pubs.acs.org/10.1021/acsmedchemlett.3c00127

Author Contributions

J.A.A., S.K., and T.H. designed the project; J.A.A. synthesized the compounds; G.W. performed the docking and ITC measurements; B.-T.B. performed ADP-Glo measurements; L.M.B. performed NanoBRET measurements; A.D.K. performed ITC measurements; A.K. provided the proteins for the DSF assay; S.K. supervised the research. The manuscript was written by J.A.A., S.K., and T.H. with contributions from all coauthors.

Notes

The authors declare the following competing financial interest(s): L.M.B. is a cofounder and B.-T.B. is a cofounder and the CEO of the Contract Research Organization CELLinib GmbH, Frankfurt, Germany.

■ ACKNOWLEDGMENTS

The authors are grateful for support by the Structural Genomics Consortium (SGC), a registered charity (no. 1097737) that receives funds from Bayer AG, Boehringer Ingelheim, Bristol Myers Squibb, Genentech, Genome Canada through Ontario Genomics Institute [OGI-196], EU/EFPIA/OICR/McGill/KTH/Diamond Innovative Medicines Initiative 2 Joint Undertaking [EUbOPEN grant 875510], Janssen, Merck KGaA (aka EMD in Canada and U.S.), Pfizer, and Takeda. B.-T.B. also received support from the collaborative research center CRC 1399 "Mechanisms of drug sensitivity and resistance in small cell lung cancer". A.K. would like to acknowledge funding from the Frankfurt Cancer Institute (FCI), an institute supported by LOEWE.

■ ABBREVIATIONS

BMP, bone morphogenetic protein; DCM, dichloromethane; DIPEA, *N,N*-diisopropylethylamine; DMF, dimethylformamide; DSF, differential scanning fluorimetry; ERK, extracellular-signal regulated kinase; HATU, hexafluorophosphate azabenzotriazole tetramethyl uronium; ITC, isothermal titration calorimetry; MAPK, mitogen-activated protein kinase; oN, overnight; rt, room temperature; SMAD, small mothers against decapentaplegic; TEA, triethylamine; TFA, trifluoroacetic acid; TGF, transforming growth factor; TKL, tyrosine kinase-like

■ REFERENCES

(1) Manning, G.; Whyte, D. B.; Martinez, R.; Hunter, T.; Sudarsanam, S. Protein Kinase Complement of the Human Genome. *Science* **2002**, *298*, 1912−1934.

(2) Gross, S.; Rahal, R.; Stransky, N.; Lengauer, C.; Hoeflich, K. P. Targeting Cancer with Kinase Inhibitors Find the Latest Version: Targeting Cancer with Kinase Inhibitors. *J. Clin. Invest.* **2015**, *125* (5), 1780−1789.

(3) Hanks, S. K. Genomic Analysis of the Eukaryotic Protein Kinase Superfamily: A Perspective. *Genome Biol.* **2003**, *4*, 111−118.

(4) Cicenas, J.; Zalyte, E.; Bairoch, A.; Gaudet, P. Kinases and Cancer. *Cancers* **2018**, *10* (3), 63.

(5) Amrhein, J. A.; Knapp, S.; Hanke, T. Synthetic Opportunities and Challenges for Macrocyclic Kinase Inhibitors. *J. Med. Chem.* **2021**, *64* (12), 7991−8009.

(6) Fang, Z.; Song, Y.; Zhan, P.; Zhang, Q.; Liu, X. Conformational Restriction: An Effective Tactic in 'Follow-on'-Based Drug Discovery. *Future Med. Chem.* **2014**, *6* (8), 885−901.

(7) Mallinson, J.; Collins, I. Macrocycles in New Drug Discovery. *Future Med. Chem.* **2012**, *4* (11), 1409−1438.

(8) Driggers, E. M.; Hale, S. P.; Lee, J.; Terrett, N. K. The Exploration of Macrocycles for Drug Discovery — an Underexploited Structural Class. *Nat. Rev. Drug Discovery* **2008**, *7*, 608−624.

(9) Johnson, T. W.; Richardson, P. F.; Bailey, S.; Brooun, A.; Burke, B. J.; Collins, M. R.; Cui, J. J.; Deal, J. G.; Deng, Y.-L.; Dinh, D.; Engstrom, L. D.; He, M.; Hoffman, J.; Hoffman, R. L.; Huang, Q.; Kania, R. S.; Kath, J. C.; Lam, H.; Lam, J. L.; Le, P. T.; Lingardo, L.; Liu, W.; McTigue, M.; Palmer, C. L.; Sach, N. W.; Smeal, T.; Smith, G. L.; Stewart, A. E.; Timofeevski, S.; Zhu, H.; Zhu, J.; Zou, H. Y.; Edwards, M. P. Discovery of (10R)-7-Amino-12-Fluoro-2,10,16-Trimethyl-15-Oxo-10,15,16,17-Tetrahydro-2H-8,4-(Metheno)-Pyrazolo[4,3-h][2,5,11]-Benzoxadiazacyclotetradecine-3-Carbonitrile (PF-06463922), a Macrocyclic Inhibitor of Anaplastic Lymphoma Kinase (ALK) and c-Ros O. *J. Med. Chem.* **2014**, *57* (11), 4720−4744.

(10) Engelhardt, H.; Böse, D.; Petronczki, M.; Scharn, D.; Bader, G.; Baum, A.; Bergner, A.; Chong, E.; Döbel, S.; Egger, G.; Engelhardt, C.; Ettmayer, P.; Fuchs, J. E.; Gerstberger, T.; Gonnella, N.; Grimm, A.; Grondal, E.; Haddad, N.; Hopfgartner, B.; Kousek, R.; Krawiec, M.; Kriz, M.; Lamarre, L.; Leung, J.; Mayer, M.; Patel, N. D.; Simov,

B. P.; Reeves, J. T.; Schnitzer, R.; Schrenk, A.; Sharps, B.; Solca, F.; Stadtmüller, H.; Tan, Z.; Wunberg, T.; Zoephel, A.; McConnell, D. B. Start Selective and Rigidify: The Discovery Path toward a Next Generation of EGFR Tyrosine Kinase Inhibitors. *J. Med. Chem.* **2019**, *62* (22), 10272−10293.
(11) Ma, J.; Sanchez-Duffhues, G.; Caradec, J.; Benderitter, P.; Hoflack, J.; ten Dijke, P. Development of Small Macrocyclic Kinase Inhibitors. *Future Med. Chem.* **2022**, *14* (6), 389−391.
(12) Liang, Y.; Fang, R.; Rao, Q. An Insight into the Medicinal Chemistry Perspective of Macrocyclic Derivatives with Antitumor Activity: A Systematic Review. *Molecules* **2022**, *27* (9), 2837.
(13) Nickel, J.; Sebald, W.; Groppe, J. C.; Mueller, T. D. Intricacies of BMP Receptor Assembly. *Cytokine Growth Factor Rev.* **2009**, *20* (5−6), 367−377.
(14) Fessel, J. P.; Loyd, J. E.; Austin, E. D. The Genetics of Pulmonary Arterial Hypertension in the Post-BMPR2 Era. *Pulm. Circ.* **2011**, *1* (3), 305−319.
(15) Chaikuad, A.; Thangaratnarajah, C.; von Delft, F.; Bullock, A. N. Structural Consequences of BMPR2 Kinase Domain Mutations Causing Pulmonary Arterial Hypertension. *Sci. Rep.* **2019**, *9* (1), 18351.
(16) Andruska, A.; Spiekerkoetter, E. Consequences of BMPR2 Deficiency in the Pulmonary Vasculature and beyond: Contributions to Pulmonary Arterial Hypertension. *Int. J. Mol. Sci.* **2018**, *19* (9), 2499.
(17) Rosenzweig, B. L.; Imamura, T.; Okadome, T.; Cox, G. N.; Yamashita, H.; Ten Dijke, P.; Heldin, C. H.; Miyazono, K. Cloning and Characterization of a Human Type II Receptor for Bone Morphogenetic Proteins. *Proc. Natl. Acad. Sci. U. S. A.* **1995**, *92* (17), 7632−7636.
(18) Xu, B.; Xu, G.; Yu, Y.; Lin, J. The Role of TGF-β or BMPR2 Signaling Pathway-Related MiRNA in Pulmonary Arterial Hypertension and Systemic Sclerosis. *Arthritis Res. Ther.* **2021**, *23* (1), 288.
(19) Kim, C. W.; Song, H.; Kumar, S.; Nam, D.; Kwon, H. S.; Chang, K. H.; Son, D. J.; Kang, D. W.; Brodie, S. A.; Weiss, D.; Vega, J. D.; Alberts-Grill, N.; Griendling, K.; Taylor, W. R.; Jo, H. Anti-Inflammatory and Antiatherogenic Role of Bmp Receptor Ii in Endothelial Cells. *Arterioscler. Thromb. Vasc. Biol.* **2013**, *33* (6), 1350−1359.
(20) Burton, V. J.; Ciuclan, L. I.; Holmes, A. M.; Rodman, D. M.; Walker, C.; Budd, D. C. Bone Morphogenetic Protein Receptor II Regulates Pulmonary Artery Endothelial Cell Barrier Function. *Blood* **2011**, *117* (1), 333−341.
(21) Pousada, G.; Lupo, V.; Cástro-Sánchez, S.; Álvarez-Satta, M.; Sánchez-Monteagudo, A.; Baloira, A.; Espinós, C.; Valverde, Di. Molecular and Functional Characterization of the BMPR2 Gene in Pulmonary Arterial Hypertension. *Sci. Rep.* **2017**, *7* (1), 1923.
(22) Derwall, M.; Malhotra, R.; Lai, C. S.; Beppu, Y.; Aikawa, E.; Seehra, J. S.; Zapol, W. M.; Bloch, K. D.; Yu, P. B. Inhibition of Bone Morphogenetic Protein Signaling Reduces Vascular Calcification and Atherosclerosis. *Arterioscler. Thromb. Vasc. Biol.* **2012**, *32* (3), 613−622.
(23) Jiramongkolchai, P.; Owens, P.; Hong, C. C. Emerging Roles of the Bone Morphogenetic Protein Pathway in Cancer: Potential Therapeutic Target for Kinase Inhibition. *Biochem. Soc. Trans.* **2016**, *44* (4), 1117−1134.
(24) Crews, L.; Adame, A.; Patrick, C.; DeLaney, A.; Pham, E.; Rockenstein, E.; Hansen, L.; Masliah, E. Increased BMP6 Levels in the Brains of Alzheimer's Disease Patients and APP Transgenic Mice Are Accompanied by Impaired Neurogenesis. *J. Neurosci.* **2010**, *30* (37), 12252−12262.
(25) Yousef, H.; Morgenthaler, A.; Schlesinger, C.; Bugaj, L.; Conboy, I. M.; Schaffer, D. V. Age-Associated Increase in BMP Signaling Inhibits Hippocampal Neurogenesis. *Stem Cells* **2015**, *33* (5), 1577−1588.
(26) Hanke, T.; Wong, J. F.; Berger, B. T.; Abdi, I.; Berger, L. M.; Tesch, R.; Tredup, C.; Bullock, A. N.; Müller, S.; Knapp, S. A Highly Selective Chemical Probe for Activin Receptor-like Kinases ALK4 and ALK5. *ACS Chem. Biol.* **2020**, *15* (4), 862−870.
(27) SGC, Chemical Probes, https://www.thesgc.org/chemical-probes.
(28) Davis, M. I.; Hunt, J. P.; Herrgard, S.; Ciceri, P.; Wodicka, L. M.; Pallares, G.; Hocker, M.; Treiber, D. K.; Zarrinkar, P. P. Comprehensive Analysis of Kinase Inhibitor Selectivity. *Nat. Biotechnol.* **2011**, *29* (11), 1046−1051.
(29) Engers, D. W.; Frist, A. Y.; Lindsley, C. W.; Hong, C. H.; Hopkins, C. R. Synthesis and Structure-Activity Relationships of a Novel and Selective Bone Morphogenetic Protein Receptor (BMP) Inhibitor Derived from the Pyrazolo[1.5-a]Pyrimidine Scaffold of Dorsomorphin: The Discovery of ML347 as an ALK2 versus ALK3 Selective MLPCN. *Bioorg. Med. Chem. Lett.* **2013**, *23* (11), 3248−3252.
(30) Modukuri, R. K.; Monsivais, D.; Li, F.; Palaniappan, M.; Bohren, K. M.; Tan, Z.; Ku, A. F.; Wang, Y.; Madasu, C.; Li, J. Y.; Tang, S.; Miklossy, G.; Palmer, S. S.; Young, D. W.; Matzuk, M. M. Discovery of Highly Potent and BMPR2-Selective Kinase Inhibitors Using DNA-Encoded Chemical Library Screening. *J. Med. Chem.* **2023**, *66*, 2143−2160.
(31) Statsuk, A. V.; Maly, D. J.; Seeliger, M. A.; Fabian, M. A.; Biggs, W. H.; Lockhart, D. J.; Zarrinkar, P. P.; Kuriyan, J.; Shokat, K. M. Tuning a Three-Component Reaction for Trapping Kinase Substrate Complexes. *J. Am. Chem. Soc.* **2008**, *130* (51), 17568−17574.
(32) Couñago, R. M.; Allerston, C. K.; Savitsky, P.; Azevedo, H.; Godoi, P. H.; Wells, C. I.; Mascarello, A.; de Souza Gama, F. H.; Massirer, K. B.; Zuercher, W. J.; Guimarães, C. R. W.; Gileadi, O. Structural Characterization of Human Vaccinia-Related Kinases (VRK) Bound to Small-Molecule Inhibitors Identifies Different P-Loop Conformations. *Sci. Rep.* **2017**, *7* (1), 7501.
(33) Fedorov, O.; Niesen, F. H.; Knapp, S. Kinase Inhibitor Selectivity Profiling Using Differential Scanning Fluorimetry. *Methods Mol. Biol.* **2012**, *795*, 109−118.
(34) Adasme, M. F.; Linnemann, K. L.; Bolz, S. N.; Kaiser, F.; Salentin, S.; Haupt, V. J.; Schroeder, M. PLIP 2021: Expanding the Scope of the Protein-Ligand Interaction Profiler to DNA and RNA. *Nucleic Acids Res.* **2021**, *49* (W1), W530−W534.
(35) Amrhein, J. A.; Berger, L. M.; Tjaden, A.; Krämer, A.; Elson, L.; Tolvanen, T.; Martinez-Molina, D.; Kaiser, A.; Schubert-Zsilavecz, M.; Müller, S.; Knapp, S.; Hanke, T. Discovery of 3-Amino-1H-pyrazole-Based Kinase Inhibitors to Illuminate the Understudied PCTAIRE Family. *Int. J. Mol. Sci.* **2022**, *23* (23), 14834.

https://doi.org/10.1021/acsmedchemlett.3c00127
ACS Med. Chem. Lett. 2023, 14, 833−840